Beach-level 24-hour forecasts of Florida red tide-induced respiratory irritation

Shane D. Ross [*,a], Jeremie Fish [b], Klaus Moeltner [c], Erik M. Bollt [b], Landon Bilyeu [d], Tracy Fanara [e,f]

[a] Aerospace and Ocean Engineering, Virginia Tech, Blacksburg, Virginia
[b] Electrical and Computer Engineering and C^3S^2 the Clarkson Center for Complex Systems Science, Clarkson University, Clarkson, New York USA
[c] Agricultural and Applied Economics, Virginia Tech, Blacksburg, Virginia USA
[d] School of Plant and Environmental Sciences, Virginia Tech, Blacksburg, Virginia USA
[e] Mote Marine Laboratory and Aquarium, Sarasota, Florida USA
[f] National Oceanic and Atmospheric Administration, Washington, DC USA

ARTICLE INFO

ABSTRACT

An accurate forecast of the red tide respiratory irritation level would improve the lives of many people living in areas affected by algal blooms. Using a decades-long database of daily beach conditions, two conceptually different models to forecast the respiratory irritation risk level one day ahead of time are trained. One model is wind-based, using the current days' respiratory level and the predicted wind direction of the following day. The other model is a probabilistic self-exciting Hawkes process model. Both models are trained on beaches in Florida during 2011–2017 and applied to the red tide bloom during 2018-2019. For beaches where there is enough historical data to develop a model, the model which performs best depends on the beach. The wind-based model is the most accurate at half the beaches, correctly predicting the respiratory risk level on average about 84% of the time. The Hawkes model is the most accurate (81% accuracy) at nearly all of the remaining beaches.

1. Introduction

Harmful algal blooms of the toxic dinoflagellate *Karenia brevis*, referred to as "Florida red tide" (henceforth abbreviated as RT) have affected the Florida Gulf coast for centuries. There is emerging evidence that these blooms have increased in frequency, intensity, and geographic spread in recent years (e.g., Alcock, 2007; Corcoran et al., 2013; Fleming et al., 2011; Nierenberg et al., 2010a; Nierenberg et al., 2010b; Nierenberg et al., 2009). *K. brevis* produces brevetoxin, a neurotoxin that can result in massive fish kills and mortalities to marine mammals and sea birds. Indirectly, this can lead to neurotoxic shellfish poisoning in humans from consuming contaminated shellfish (Corcoran et al., 2013; Kirkpatrick et al., 2006).

More directly, and of primary interest for this study, brevetoxin is released into near-shore aerosol as RT cells are lysed by wave action, or aerosolized though bubble-mediated (Pietsch et al., 2018) transport. If inhaled by humans, brevetoxin can produce upper and lower respiratory irritation, such as a burning sensation of eyes and nose, and a dry, choking cough. While these symptoms have been found to be relatively short-lived in healthy individuals (upon separation from the harmful aerosol), RT effects can be more severe and longer-lasting for people with chronic respiratory conditions, such as asthma (Alcock, 2007; Backer et al., 2003; Corcoran et al., 2013; Fleming et al., 2011; Kirkpatrick et al., 2009; 2011; Nierenberg et al., 2010b).

In this study, the potential of forecasting beach-specific respiratory irritation one day ahead of time is assessed, using previous irritation reports at the same location. Two models are proposed: one based on the current respiratory irritation level and a forecast of the next day's wind direction, and the other based on RT as a self-exciting process (or Hawkes process). Both are data-driven, trained on data on from 2011–2017, and tested on data from a severe RT bloom during 2018-2019. Both are compared with a simple persistence model, which assumes the next day's respiratory irritation level will be the same as the current day's.

---

* Corresponding author.
  E-mail address: shaneross@vt.edu (S.D. Ross).

1.1. Monitoring of red tide blooms

Monitoring for *K. brevis* blooms involves the following primary components. Satellite imagery is processed to locate potential blooms. Processed images are made available to managers and state health officials in the Gulf of Mexico through the National Oceanic and Atmospheric Administration (NOAA) Harmful Algal Bloom Operational Forecast System (HAB-OFS) (National Oceanic and Atmospheric Administration, 2021). In Florida, where blooms tend to occur most frequently, water samples are collected weekly along the shore and from offshore transects by the Florida Fish and Wildlife Research Institute once a bloom is identified. Samples are delivered to a laboratory for cell enumeration via microscopy. Microscopic enumeration takes about one hour per sample (Hardison et al., 2019). Typically, samples are processed within 12 days and can take longer for more samples from remote areas. The resulting cell counts are then used by HAB-OFS to provide broad, county-wide forecasts of brevetoxin exposure risks. The cell count data for a particular county can be up to a week old by the time it is available to the public. In terms of forecast accuracy, (Stumpf et al., 2009) found that while county-wide forecasts of respiratory risk were correct 70% of the time, they were only correct 20% of the time when applied to individual beaches.

Recently, beach-level 24-hour forecasts for respiratory impacts have received the most focus from policy agencies (Moeltner et al., 2021). The Gulf of Mexico Coastal Ocean Observing System (GCOOS) recently developed a beach-level risk forecast that includes more than 20 Gulf Coast beaches (System, 2021). The forecast uses current wind forecasts as well as near real-time cell counts of *K. brevis* from water samples enabled by HABscope, a portable microscope system (Hardison et al., 2019). While the beach reporting system described below provides different data (actual beach-level respiratory impact, collected daily over several years), one can envision the potential to tie in to existing forecast frameworks, fusing the multiple data sources for more accurate forecasts or greater spatial coverage.

1.2. Beach conditions reporting system

To address the need for location-specific conditions, a Beach Conditions Reporting System (BCRS) was initiated in 2006 (Currier et al., 2009; Kirkpatrick et al., 2008; Nierenberg et al., 2011; Stumpf et al., 2009) and was redeveloped in 2015 when it began gaining public usership (Mote Marine Laboratory & Aquarium, 2021). From 2017-2019, the site gained approximately 1.5 million users. The BCRS provided smartphones to (professional) lifeguards and park rangers with an app designed for reporting beach conditions. Twice each day (10:00 and 15:00 local time), lifeguards and park rangers report occurrence of coughing as described further below (and other conditions such as presence of dead fish). While lacking the quantification and precision of microscopy, the reports provide beachgoers with useful real-time information for adequate planning (i.e., severity of aerosolized toxins, potential risks to asthmatics, presence of dead fish, etc.). The BCRS is managed by Mote Marine Laboratory with lifeguards and park rangers as the primary reporters in several counties (Mote Marine Laboratory & Aquarium, 2021). The BCRS data compilation is automated, with timely sharing of data with agencies, including Florida Fish and Wildlife Conservation Commission and NOAA.

Though the BCRS provides more timely information about beach conditions than the weekly sampling described earlier, it does not provide key information needed for consistent forecasts. It provides no direct information on *K. brevis* cell presence, but rather an indirect assessment of *K. brevis* cell presence via water color and the presence of dead fish.

While RT outbreaks can occur throughout the entire year, aerosolized RT impacts have shown substantial variability both in a temporal and spatial sense. They can last from a few hours to multiple days or even weeks at a given site (e.g., beach), and vary in intensity across sites

Table 1
The four-tiered red tide respiratory irritation levels reported in the Beach Conditions Reporting System, and the corresponding two-tiered risk level defined for this study.

Irritation level	Risk level	In a 30 s audio sample
None	Low	No coughing/sneezing heard in 30 s
Slight	Low	A few coughs/sneezes heard in 30 s
Moderate	High	A cough/sneeze heard every 5 s
High	High	Coughing/sneezing almost continuously

at a given point in time, with heavily impacted areas at times alternating with completely unaffected shoreline segments (Nierenberg et al., 2009).

While efforts are ongoing to curb RT blooms via prevention and control methods (Alcock, 2007; Kirkpatrick et al., 2014; Nierenberg et al., 2010a; Vargo et al., 2008), the predominant management strategy to date has been mitigation, via early detection and avoidance of human contact (Alcock, 2007; Corcoran et al., 2013).

2. Methods

Below, the RT respiratory irritation data set is described. Afterward, two different models to predict RT irritation risk one day ahead of time are described: a wind-based model and a Hawkes process model.

2.1. Respiratory irritation data

Starting in August 2006, the professional lifeguard corps in Sarasota County began twice-daily reports (approx. 10:00 and 15:00 local time) of the presence of respiratory irritation at six sites, as part of the BCRS. In January 2007, two additional lifeguard sites were added in Manatee County. Respiratory irritation is defined by the amount of coughing observed in addition to the personal conditions experienced by the lifeguard. The presence of people coughing is used as a proxy for respiratory irritation (cough, nasal congestion, throat irritation, chest tightness, wheezing, and shortness of breath). Coughing has been documented as a response to *K. brevis* aerosols in studies involving occupationally exposed workers, recreationally exposed beachgoers, and asthmatics (Backer et al., 2003; 2005; Fleming et al., 2005; 2007).

Lifeguards 'listen' to beachgoers for the presence and/or frequency of coughing. The symptoms observed by the lifeguards are reported at various levels of respiratory irritation as shown in Table 1.

Irritation levels are given on a four-tiered scale from 'None' (no coughing noted nearby), 'Slight' (a few coughs and sneezes within 30 s), 'Moderate' (A cough/sneeze heard every 5 s), and 'High' (continuous coughing and sneezing in nearby surroundings). For portions of the analysis below, moderate and high classes are together as 'high' risk, as these were the level at which impacts affect the general public Stumpf et al. (2009). The 'none' and 'slight' are grouped as 'low' risk. The two-tiered (binary) classification of RT respiratory irritation risk was used in this study for an initial analysis of forecasting methods, based on historical data.

2.2. Statistics describing the data set

Since December 2011, the BCRS has monitored RT conditions at over 40 beaches in nine counties along the Gulf coast via citizen scientists, in most cases local lifeguards. This study considered only the time frame when 40 beaches were reporting. The eight beaches which are the focus of this study (see Fig. 1) were chosen because they were the only beaches with enough reports of high respiratory risk days to develop a convergent model, as described below.

Figure 2 shows the annual aggregate sum of RT irritation reports (level 'slight' or higher) from the six beaches in Sarasota County. It is clear that in 2018, the county was especially hard-hit by RT.

Fig. 1. Eight beaches along the Florida Gulf Coast out of 40 for which reporting is available from 2011-2019. These eight have the highest number of reported red tide respiratory events: six are in Sarasota County and two are in Manatee County.

For the purposes of the model, only the highest daily irritation level is considered. Reports are given twice per day, separated by only a few hours, and are often the same. When they differ, the higher of the four-tiered irritation level is used to describe the risk-level for that day. For the two-tiered irritation risk of high and low, there was near unanimous agreement between the two daily reports.

Correlation of irritation level across distance and time. From the BCRS database, correlation of the respiratory irritation level with nearby beaches is considered. For the four-tier irritation levels described as None to High (see Table 1), numerical values 1 through 4 were assigned, respectively. As one can see in the left panel of Fig. 3, the correlation of nearby beaches (within a few km) is high,

but drops off to about 50% for beaches from 5 km up to approximately 25 km away, decreasing approximately monotonically with distance. One can also consider the correlation of irritation level across time for an individual beach. The average auto-correlation of a beach's respiratory irritation level versus time-lag is reported. Notice there is a moderate correlation for 1 day, but the correlation drops to about zero

after 2 days. These spatiotemporal correlations are reported merely to describe the data set. They are not incorporated into the models described below.

2.3. Partition of data into training and testing sets

The BCRS database contains respiratory irritation reports from December 2011 to April 2019. Following standard practice in machine learning (Brunton and Kutz, 2019), a data set must be partitioned into a training and testing set. A model is constructed from the training set and validated on the testing set. Training on earlier data in order to test on later data is a common method as it mimics forecasting, and this approach will be followed in the current study. The data reveal that there was a time-frame of a significant number of reports during 2018 until early 2019 (Fig. 2). The 2018-2019 time-frame therefore emerges as a testing data set. All earlier data, from 2011-Dec-31 to 2017-Dec-31, are considered as the training data set.

The database has long stretches of no respiratory irritation reports
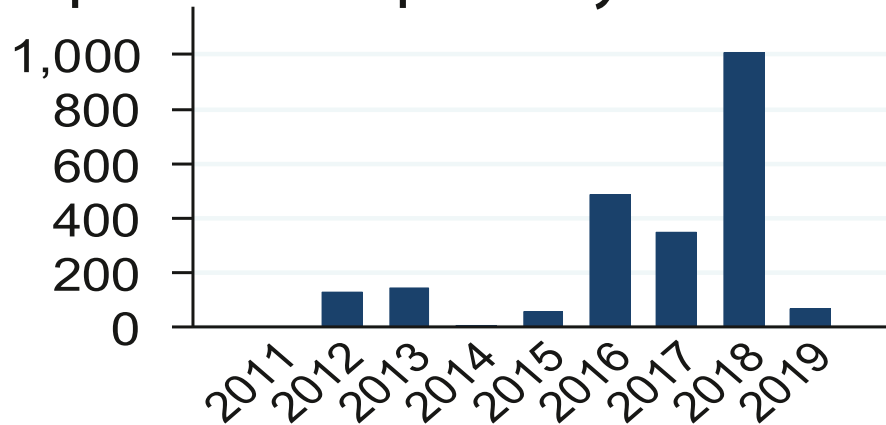
Reports of respiratory irritation

Fig. 2. Reports of respiratory irritation caused by red tide for Sarasota County, from December 2011 to April 2019.
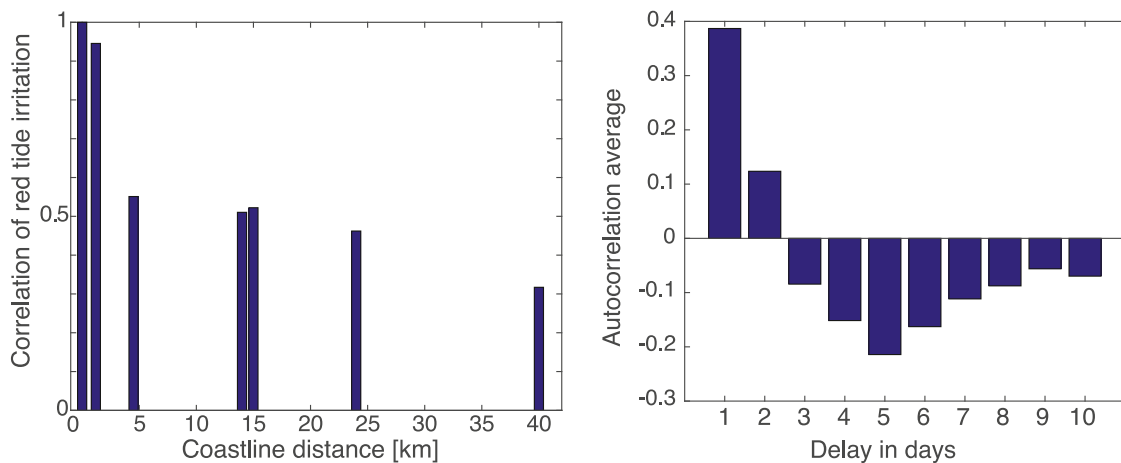

Fig. 3. (left) Correlation of red tide respiratory irritation level between the different beaches in Fig. 1 as a function of coastline distance. (right) The average auto-correlation of a beach's red tide respiratory irritation level with time.

(that is, recorded as None). For forecasting purposes, the ability to predict respiratory irritation during a cluster of such events is a primary focus of this study. To be precise, a *red tide respiratory irritation episode* is defined on a beach-by-beach basis for all data as follows. A RT respiratory irritation episode is said to begin the day when the BCRS irritation report (see Table 1) first goes above None and ends 7 days after the last irritation report above None.

2.4. Wind-based model

The wind direction reported from the BCRS at each beach was given as one of the eight usual directional octants of width 45° (N, NE, E, SE, S, SW, W, and NW). For the beaches of interest on the west coast of Florida, onshore winds were defined as winds blowing from 168.75° to 326.25° (S clockwise to NW, following Stumpf et al., 2003; Stumpf et al., 2009), which presumes the 330° to 150° orientation of the coastline, as shown in Fig. 4.

It is noted that the beach coastlines do not deviate enough from this assumed coastline for the coarseness of the input wind direction to make a difference in modeling.

For a wind-based model, the following statistical analysis from the BCRS database is performed for the training set (years 2011–2017), restricted only to RT respiratory irritation periods. For a respiratory irritation level of r_t on day t, where $r_t \in$ {None, Slight, Moderate, High},

the probability of r_{t+1} on day $t+1$ is calculated, based on the frequencies of such occurrences in the database. Two conditions are considered: onshore winds on day $t+1$ and offshore winds on day $t+1$. The results are shown in Fig. 5.

For instance, if today's respiratory irritation level is Moderate, and there will be onshore winds tomorrow, then with over 60% probability, tomorrow's irritation level will be Moderate or High (high risk). On the other hand, if tomorrow's winds are offshore, then with about 60% probability the irritation level will improve, to Slight or None (low risk).

If this probability distribution is assumed to hold for future events, then one has a straightforward forecast model for the respiratory irritation level based on the weather forecast, in particular, the wind direction forecast. To get a deterministic model in place of a probabilistic model, one can assume that the state with the maximum likelihood is the one which occurs. This leads to the simple model given in Fig. 6.

For instance, if the irritation level today is at None, but tomorrow has onshore winds, the maximum likelihood is that it will be Slight tomorrow, since the light-blue bar in the first stack of the left panel of Fig. 5 is longer than all others. In place of the four-tiered irritation level, one can use the simpler two-tiered irritation risk level, low and high, as given in Table 1. This coarser, binary description of the irritation level is used as it is more amenable to modeling and validation.
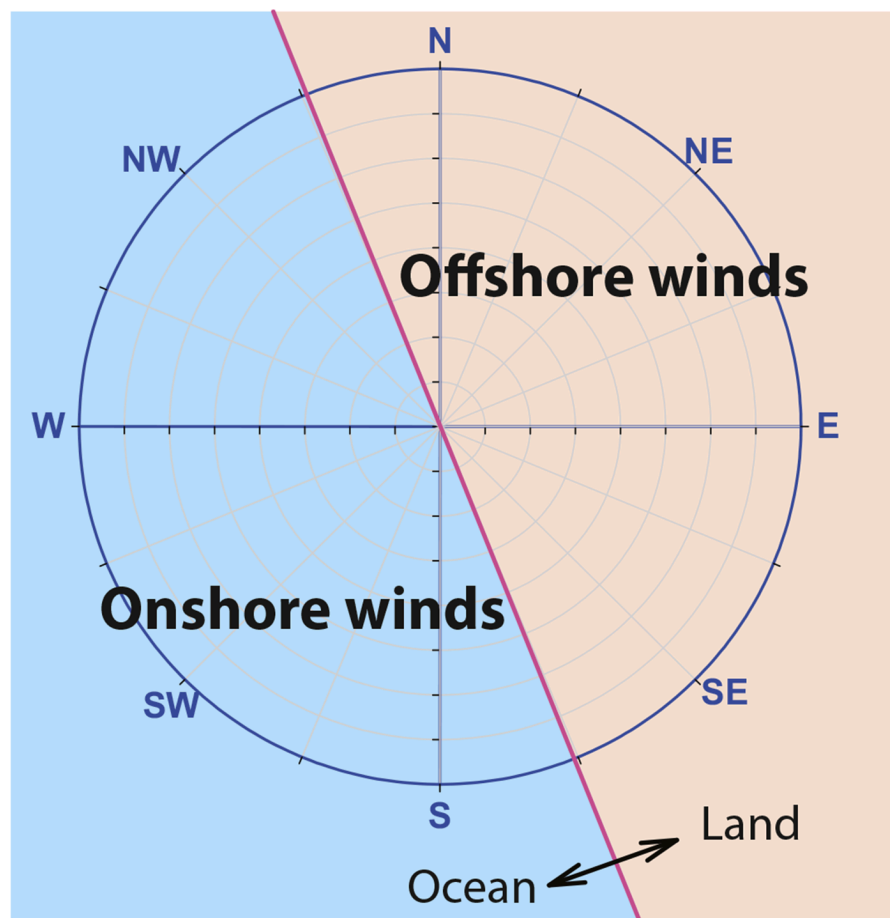
Fig. 4. Definition of onshore and offshore wind directions for the beaches studied. The standard wind direction convention is used, where direction denotes where the wind is coming from.
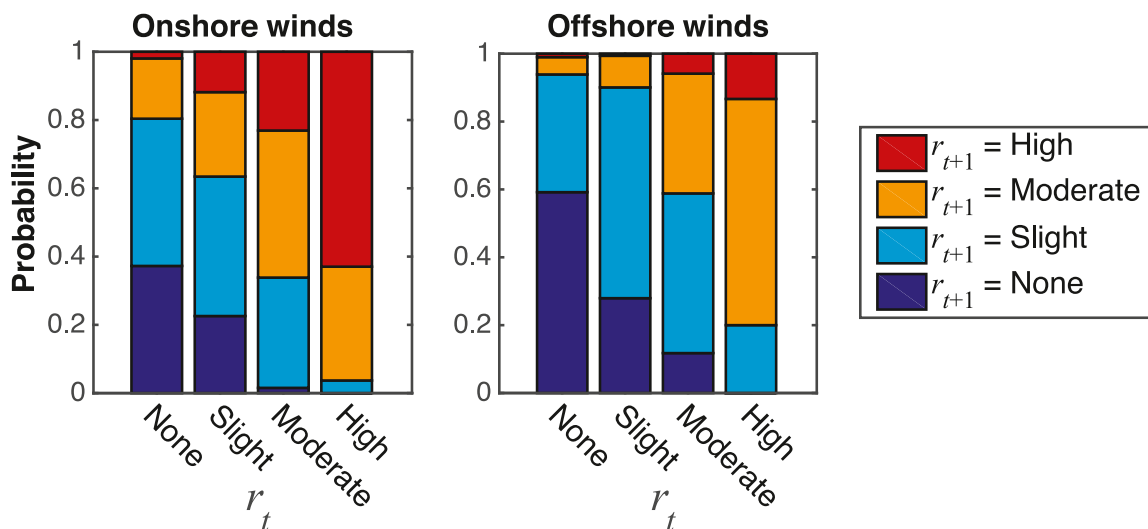

Fig. 5. Respiratory irritation level on day $t + 1$ as a function of the level on day t and the wind condition on day $t + 1$; onshore or offshore winds.

2.5. Hawkes process model

Hawkes processes have been used to model a remarkable range of phenomena. From earthquakes (Ogata, 1988; Türkyilmaz et al., 2013), to gang related violence (Mohler et al., 2011; Park et al., 2021) to econometrics (Bacry et al., 2013; Errais et al., 2010). This type of model performs well in situations where there is evidence for a clustering of events in time.

Hawkes processes are a type of temporal point process. The classic temporal point process is the *homogeneous* Poisson process, an example of which is the number of asteroids striking the Earth. Presumably the probability of an asteroid strike is independent of whether or not there was a previous strike. Poisson processes are thus "memoryless" and events are roughly equally spaced in time. An illustrative example of a
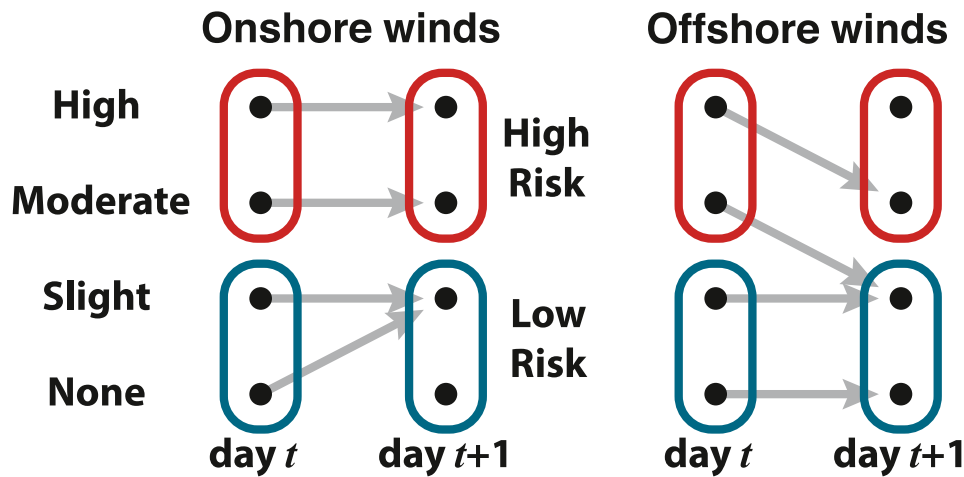
Fig. 6. Wind-based respiratory irritation model.

homogeneous Poisson process compared to a non-homogeneous (Hawkes) Poisson process is provided in Appendix A.

A homogeneous Poisson process is a stochastic point process in which events happen with *constant* rate λ and with probability,

$$P_{\text{Poisson}}(k|\lambda) = \frac{(\lambda t)^k}{k!} e^{-\lambda t}, \tag{1}$$

where λ has units of inverse time. A *non-homogeneous* Poisson process is one in which the rate parameter $\lambda(t)$ is a function of time. A linear Hawkes process with an exponential kernel (Hawkes, 1971) is a non-homogeneous Poisson process where,

$$\lambda(t) = \lambda_0 + \sum_i \alpha e^{-\beta(t-\tau_i)}. \tag{2}$$

where $\lambda_0 \geq 0$ is the background intensity rate, $\alpha > 0$ is the excitation level, $\beta > 0$ is the reversion level, and $\{\tau_1, \tau_2, ...\tau_i\}$ is the observed true sequence of past event times (high risk days in the current study).

A Hawkes process is known as a *self-exciting process* because when an excitation happens the rate increases before decaying to the natural unexcited rate λ_0 (see Appendix A). The rate initially increases by the amount α when an event arrives but exponentially decays with rate β towards λ_0. The Hawkes process maintains a finite rate $\lambda(t)$ so long as $\alpha < \beta$ (Laub et al., 2015).

Estimation of the parameters for the Hawkes process is done via maximum likelihood estimation (MLE) of Fisher (1922), a procedure for estimating model parameters from a training set such that the observed data is most probable (Brunton and Kutz, 2019). Details of MLE for a Hawkes process can be found in Appendix B. For each beach, the parameters λ_0, α, β, and $P_{\text{threshold}}$ are estimated based on the training data set for that beach. If the parameters converge to the same values independent of random initial parameters in the MLE process, the Hawkes model has *converged*. Only beaches which have a convergent Hawkes model are included in the Results. It is expected that not all, or even a majority of the beaches will have convergent Hawkes models, as it is known that for some types of data, parameter estimation is quite sensitive to the random initial guess (Veen and Schoenberg, 2008).

Once the parameters $\{\lambda_0, \alpha, \beta, P_{\text{threshold}}\}$ have been estimated for a given beach, the probability of observing no events (high risk days) at each time is determined by substituting $\lambda(t)$ into Eq. (1), where $\lambda(t)$ is given by Eq. (2). This gives, on each day t, the probability of the next day, $\Delta t = 1$ d, being a high risk day, which is $1 - P_{\text{Poisson}}(0|\lambda(t))$, that is,

$$P_{\text{highrisk}}(t) = 1 - e^{-\lambda(t)\Delta t}. \tag{3}$$

The model predicts that the next day, $t + 1$, will be a high risk day if

Table 2
Estimated values of the Hawkes parameters for each of the beaches considered, listed north to south. Units of λ_0, α, and β are inverse days, d^{-1}. The bottom rows shows the average parameter value (across all beaches) along with the standard deviation.

Beach	λ_0	α	β	$P_{\text{threshold}}$
Manatee	0.0027	0.2393	0.3151	0.2932
Coquina	0.0039	0.3181	0.4016	0.3451
Lido	0.0054	0.1324	0.2332	0.2600
Siesta	0.0059	0.2370	0.3700	0.3680
Nokomis	0.0041	0.1039	0.1218	0.3137
Venice North	0.0058	0.1457	0.1917	0.3211
Venice	0.0052	0.1449	0.2404	0.2785
Manasota	0.0049	0.2219	0.3182	0.3350
Average	0.0047	0.1929	0.2740	0.3143
(Standard Deviation)	(0.0011)	(0.072)	(0.094)	(0.036)

$$P_{\text{highrisk}}(t) > P_{\text{threshold}}. \tag{4}$$

3. Results

The Hawkes process model parameter estimation was performed for the training data (years 2011-2017) at all 40 beaches in the BCRS database. The parameter estimation process converged at only 8 of the 40 beaches. They were located in a geographic cluster (see Fig. 1) and from north to south are Manatee, Coquina, Lido, Siesta, Nokomis, Venice North, Venice, and Manasota. The set of parameters are calculated independently for each beach, and reported in Table 2.

In all the beaches examined, the parameter $\beta \approx 0.27$ d^{-1}, which suggests a correlation time-scale of $\beta^{-1} \approx 3.6$ days. A longer probabilistic "memory" timescale can be estimated,

$$T_m = -\log(0.05)/\beta + 1 \quad \text{(in days)}, \tag{5}$$

which is about 12 days, since a high risk day which happened 12 days ago has a contribution of about 5% compared to that of high risk day which occurred 1 day ago. Also of interest is that the estimates show that $\alpha \approx 0.2$ d^{-1} for all beaches. This is roughly 10^3 times the base rate, $\lambda_0 \approx 0.005$, for each beach, meaning that a single high risk day after several low risk days increases the probability of more high risk days by several orders of magnitude.

The wind-based and Hawkes process models were applied to the test data at each of the eight beaches for which a convergent Hawkes process model was found. For comparison, a persistence model is included as a null hypothesis. The persistence model assumes that tomorrow will be

Table 3

For each beach, the percent of days for which the respiratory irritation risk was correctly forecast by each model during the dates shown is reported as the accuracy. Also given are the false negative rate (also called the miss rate) and the false positive rate.

Beach and Time-frame	Model	Accuracy	False Negative Rate	False Positive Rate
Manatee, 181 days 2018-Aug-03 to 2019-Jan-30	Persistence	77%	44%	16%
	Wind	78%	69%	5%
	Hawkes	80%	42%	13%
Coquina, 181 days 2018-Aug-03 to 2019-Jan-30	Persistence	75%	46%	18%
	Wind	75%	68%	9%
	Hawkes	78%	44%	14%
Lido, 239 days 2018-Jun-06 to 2019-Jan-30	Persistence	85%	36%	10%
	Wind	83%	62%	5%
	Hawkes	83%	56%	6%
Siesta, 237 days 2018-Jun-08 to 2019-Jan-30	Persistence	83%	36%	12%
	Wind	84%	43%	8%
	Hawkes	85%	46%	6%
Nokomis, 239 days 2018-Jun-06 to 2019-Jan-30	Persistence	80%	44%	13%
	Wind	82%	60%	5%
	Hawkes	74%	65%	14%
Venice North, 239 days 2018-Jun-06 to 2019-Jan-30	Persistence	80%	43%	13%
	Wind	81%	61%	6%
	Hawkes	75%	64%	13%
Venice, 238 days 2018-Jun-05 to 2019-Jan-22	Persistence	79%	47%	13%
	Wind	85%	53%	4%
	Hawkes	78%	59%	11%
Manasota, 232 days 2018-Jun-07 to 2019-Jan-30	Persistence	81%	43%	13%
	Wind	87%	48%	3%
	Hawkes	78%	57%	11%

like today. The results are reported in Table 3.

For each beach and each model, the accuracy is reported, or the percent of days for which the respiratory irritation risk was correctly forecast. Also given are the false negative rate (also called the miss rate) and the false positive rate.

Considering only the accuracy, the model which performs the best depends on the beach. For the two northern-most beaches and Siesta, the Hawkes model is the most accurate. For the four southern-most beaches, the wind model performs best. Only at Lido does the simple persistence model perform best. But notice that even when a model is the most accurate, it might not have the lowest false negative rate, or percent of true high risk days that were not predicted. At all but the two northern-most beaches, persistence has the lowest false negative rate. At all but one beach (Siesta), the wind model has the lowest false positive rate (predicting a high risk day which is in fact low risk).

The self-excitation behavior characteristic of the Hawkes process can be seen in the example of Coquina Beach, Fig. 7.

The probability of the following day being high risk is a function of all actual high risk days in the recent past. When the probability exceeds the threshold, the model predicts the following day will be high risk day. For this beach, the Hawkes model had the highest accuracy. The wind and persistence models are shown for comparison. Results for Venice Beach are also shown, an example where the wind model had the highest

accuracy, in Fig. 8.

4. Discussion

The BCRS has accumulated a significant amount of data since its launch in 2006. In the absence of a more sophisticated first-principles-based forecasting system, the historical data could be utilized to provide a near-term beach-level forecast at the locations considered. For forecasting the beach-specific respiratory irritation risk level one day ahead of time, all the models perform similarly during the 2018-2019 RT respiratory irritation episode, between 75% and 85% accuracy (see Table 3). The simple persistence model (tomorrow will be like today) does rather well, near 80% accuracy, and at one beach (Lido), was the best performer. The wind-based model is the most accurate for half the beaches for which a model was developed. All were geographically located near each other, in the southern part of Sarasota County.

Interestingly, the probabilistic self-exciting Hawkes process model, which does not contain wind as an input, outperforms the more intuitive wind-based model at nearly half of the beaches. Fortuitously, there were enough events to get numerical estimates for the parameters of a univariate Hawkes process, but not enough for a multivariate analysis (i.e., including wind data). With additional data containing high-risk events, adding wind data to the Hawkes process model may be possible. That is, a hybrid of the models considered here could potentially improve accuracy, but the amount of historical data available to train the model would need to increase significantly.

Limitations. The given models do not predict when a RT bloom will occur, or when a RT respiratory irritation episode will occur at any given beach. However, when a RT respiratory irritation episode does begin, the models provide a method for forecasting the respiratory irritation risk for the next day, based on the recent risk history.

Data for all 40 beaches goes back only to December 2011. The total number of high risk days during the 2,193-day training period ranges from a low of zero to a high of 46. Among the eight beaches for which a model was developed, high risk days account for only about 1% of the training period. This is very little data for which to train a model. With more data, the Hawkes and wind models may improve.

Data from different blooms were lumped together to get enough data to train the models. Yet RT blooms are known to be patchy and highly variable from bloom to bloom. Thus, the training data may combine behavior from different blooms with different dynamics. This is a limitation of the data set used.

To simplify the modeling, the four-tiered respiratory irritation scale was coarsened into a two-tiered risk scale (Table 1). Ideally, respiratory irritation could be measured on a continuous scale, using for example sensors for automatic cough detection and counting at beaches. Modeling of a continuous variable would increase the number of available data-driven modeling methods.

5. Conclusions

The Beach Condition Reporting System (BCRS) which has been operational for over a decade, has accumulated a wealth of data. In particular, red tide-induced respiratory irritation levels at individual beaches have been reported daily over this time period. The analysis performed here provides one of the first reports of the statistics of this data set.

Moreover, beach-level next-day forecasts of the respiratory irritation risk were developed on a beach-by-beach basis, if there was enough data in the training set for a model to be developed. Training on data from red tide respiratory irritation episodes during the time period 2011–2017, only eight beaches had enough data for a model to be developed (i.e., for parameter values for the probabilistic Hawkes model to converge). Two types of models provided a forecast of the respiratory level 24-hours ahead of time during the extensive red time bloom of 2018-2019, and were compared with a simple persistence model. One model was wind-
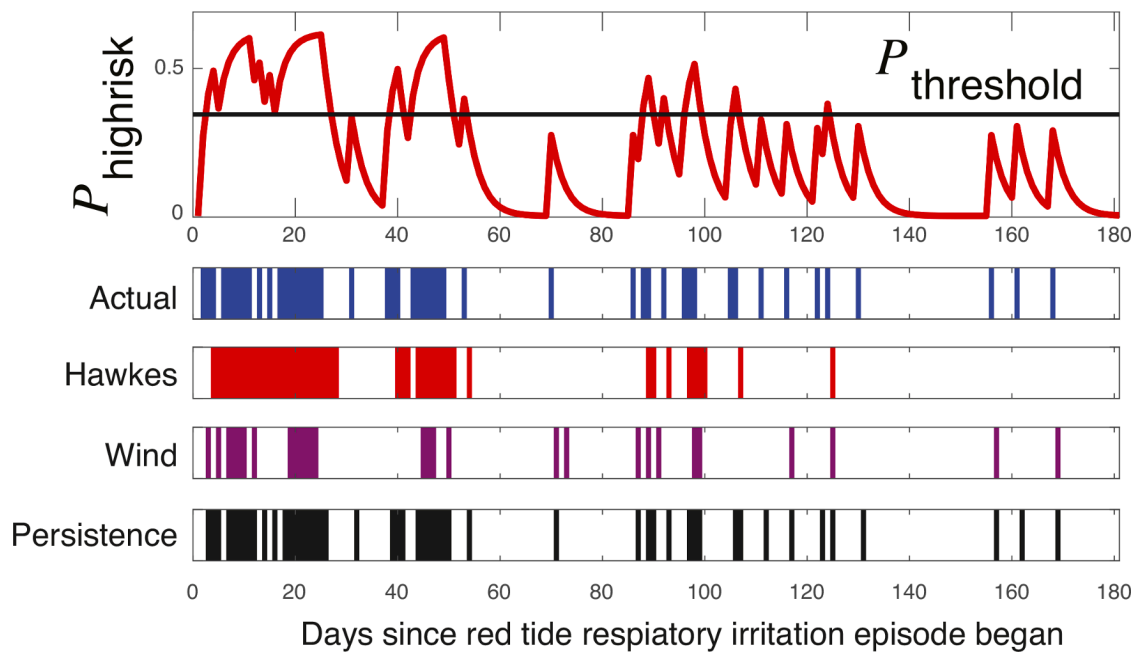
Fig. 7. For Coquina Beach, Manatee County, Florida, the days of actual high respiratory risk level are shown, and several 1-day forecast models, during the red tide respiratory irritation episode that began August 2018. The probability of a high risk day using the Hawkes process model is shown at top. The flat black line represents the threshold. When the probability of a high risk day exceeds the threshold, the day is forecast as a high risk day. Otherwise, it will forecast as a low risk day. The Hawkes model performs best in this case. The wind-based and persistence models are shown for comparison.
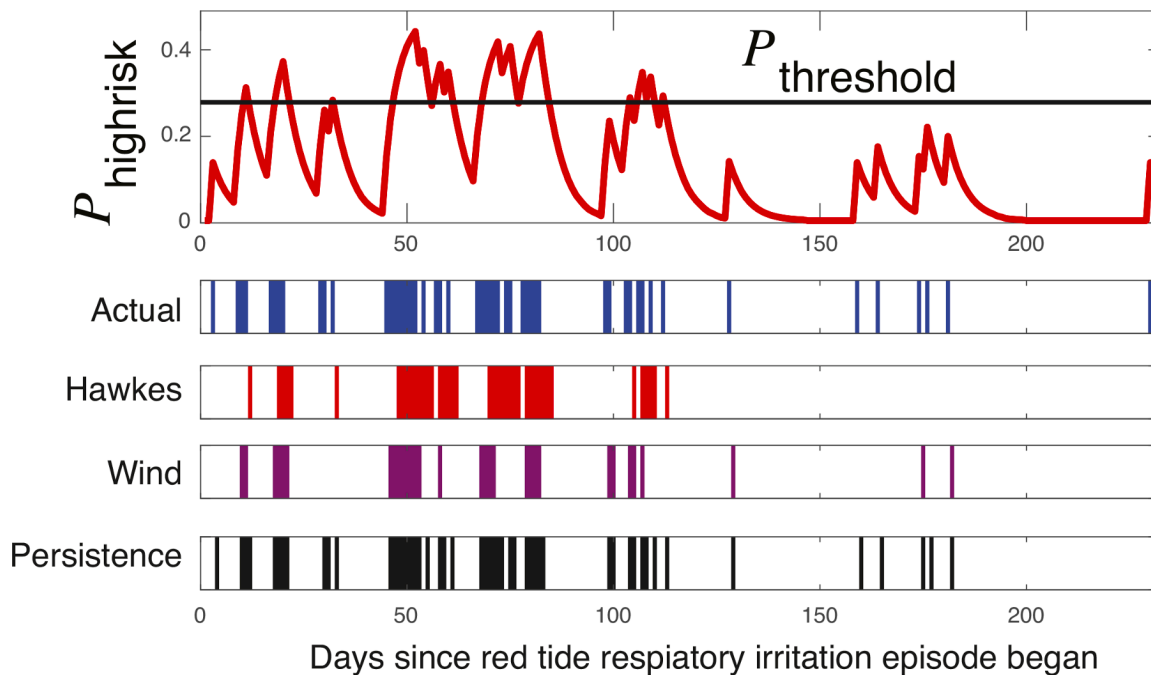
Fig. 8. Same data as in Fig. 7 but for Venice Beach, Sarasota County, Florida during the red tide respiratory irritation episode that began June 2018. The wind model performs best in this case.

based, using the current days' respiratory level and the predicted wind direction of the following day. The other model was a probabilistic self-exciting Hawkes process model, which used as input the record of the recent risk history.

No single model performed the best at all the beaches. The wind-based model performed the best at four of the eight beaches, correctly predicting the respiratory risk level an average of 84% of the time. At three of the eight beaches, the Hawkes model was the most accurate, accurately predicting the next day's risk level an average of 81% of the time. At one beach, the persistence model outperformed both the wind and Hawkes models, with an accuracy of 85%. The accuracy of the Hawkes process model at nearly half the beaches for which a model was developed suggests it may be fruitful to consider self-excitation-based approaches in larger-scale models of harmful algal blooms. Interestingly, the Hawkes process model does not require water samples of *K. brevis*, nor ocean or wind forecasts, and will likely improve by their inclusion.

These results suggest that beach-level on-site reports of respiratory irritation are a valuable data source, providing an excellent means to forecast the following day's beach-specific respiratory irritation risk at the same location. Moreover, the efficacy of the BCRS suggests that timely and regular reports of red tide-induced respiratory irritation level should continue to be supported and should be incorporated in operational forecasts used by resource managers and the public.

Declaration of Competing Interest

Acknowledgements

Appendix A. Example Hawkes process

A homogeneous Poisson process (with constant rate $\lambda = 1$) is shown in the bottom of Fig. A.9. The Hawkes process by contrast is a type of non-homogeneous Poisson process, in which the rate of events are dependent upon the history of arrivals and the time which has passed between events. The probability of seeing a new event, e.g., a high risk day, increases when a previous event has occurred. This leads to the temporal clustering seen in the middle panel of Fig. A.9. A more detailed description of a Hawkes process is provided in Section 2.5.
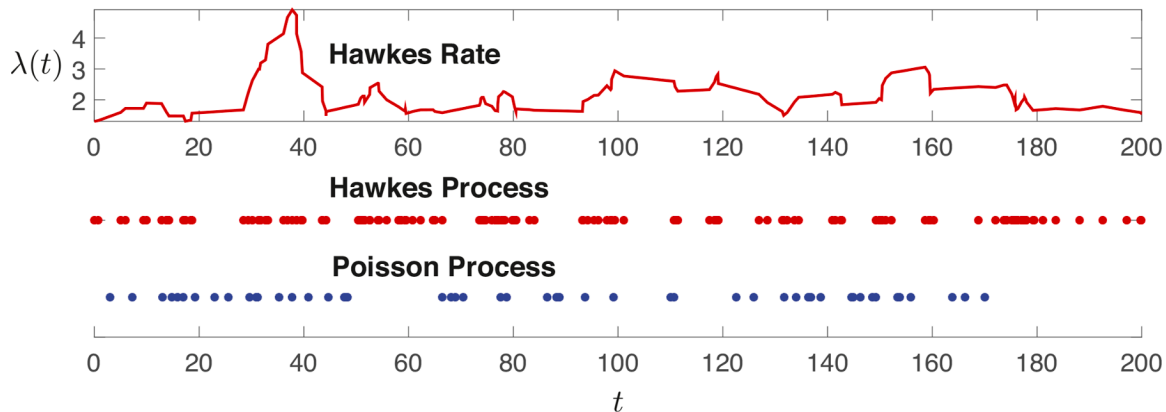

Fig. A1. The varying rate of an example Hawkes process can be seen (top). A Hawkes process (middle) tends to have events which cluster in time, whereas a Poisson process with the same initial rate (bottom) produces events that are roughly equally spaced in time. The Hawkes process proves to be a good model for many natural processes, which also tend to have events which cluster in time.

Appendix B. Hawkes maximum likelihood estimation

The parameters α, β, λ_0, and $P_{\text{threshold}}$ may be estimated via maximum likelihood estimation (MLE). The log-likelihood function of the Hawkes process is given by Ozaki (1979):

$$\mathscr{L}(\tau_1, ..., \tau_n | \alpha, \beta, \lambda_0) = -\lambda_0 T + \sum_{i=1}^{n} \frac{\alpha}{\beta} \left[e^{-\beta(T - \tau_i)} - 1 \right] + \sum_{i=1}^{n} \log(\lambda_0 + \alpha A(i)), \tag{B.1}$$

where T is the total time which has been recorded,

$$A(i) = \sum_{\tau_i > \tau_j} e^{-\beta(\tau_i - \tau_j)} \ (\forall i \geq 2) \tag{B.2}$$

and τ_n is the time of the last recorded *event*. One may find the partial derivatives of the log likelihood function given in Eq. (B.1) in Ozaki (1979). However, estimation of the maximum (by setting the partial derivatives equal to zero and solving) is challenging. So as an alternative, standard numerical techniques for nonlinear optimization can be used, in this case the Nelder-Mead direct search technique (Nelder and Mead, 1965) to estimate the parameters.

References

Alcock, F., 2007. An assessment of Florida Red Tide: Causes, Consequences and Management Strategies. Technical report 1190. Mote Marine Laboratory.

Backer, L.C., Fleming, L.E., Rowan, A., Cheng, Y.-S., Benson, J., Pierce, R.H., Zaias, J., Bean, J., Bossart, G.D., Johnson, D., Quimbo, R., Baden, D.G., 2003. Recreational exposure to aerosolized brevetoxins during Florida red tide events. Harmful Algae 2, 19–28.

Backer, L.C., Kirkpatrick, B., Fleming, L.E., Cheng, Y.S., Pierce, R., Bean, J.A., Clark, R., Johnson, D., Wanner, A., Tamer, R., Zhou, Y., Baden, D.G., 2005. Occupational exposure to aerosolized brevetoxins during Florida red tide events: effects on a healthy worker population. Environ. Health Perspect. 113, 644–649.

Bacry, E., Delattre, S., Hoffmann, M., Muzy, J.F., 2013. Modelling microstructure noise with mutually exciting point processes. Quant. Finance 13, 65–77.

Brunton, S.L., Kutz, J.N., 2019. Data-Driven Science and Engineering: Machine Learning, Dynamical Systems, and Control. Cambridge University Press.

Corcoran, A., Dornback, M., Kirkpatrick, B., Jochens, A., 2013. A Primer on Gulf of Mexico Harmful Algal Blooms. Technical Report. Gulf of Mexico Alliance & Gulf of Mexico Coastal Ocean Observing System.

Currier, R. D., Boyes, C., Hails, A., Nierenberg, K., Kirkpatrick, B., & Kirkpatrick, G. (2009). An ocean observing system for harmful algal bloom detection and tracking. IEEE. OCEANS 2009, 1–4.

Errais, E., Giesecke, K., Goldberg, L.R., 2010. Affine point processes and portfolio credit risk. SIAM J. Financ. Math. 1, 642–665.

Fisher, R.A., 1922. On the mathematical foundations of theoretical statistics. Philos. Trans. R. Soc.London Ser. A 222, 309–368.

Fleming, L.E., Kirkpatrick, B., Backer, L.C., Bean, J.A., Wanner, A., Dalpra, D., Tamer, R., Zaias, J., Cheng, Y.S., Pierce, R., Naar, J., Abraham, W., Clark, R., Zhou, Y., Henry, M.S., Johnson, D., Bogart, G.V.D., Bossart, G.D., Harrington, M., Baden, D.G., 2005. Initial evaluation of the effects of aerosolized Florida red tide toxins (brevetoxins) in persons with asthma. Environ. Health Perspect. 113, 650–657.

Fleming, L.E., Kirkpatrick, B., Backer, L.C., Bean, J.A., Wanner, A., Reich, A., Zaias, J., Cheng, Y.S., Pierce, R., Naar, J., Abraham, W.M., Baden, D.G., 2007. Aerosolized red-tide toxins (brevetoxins) and asthma. Chest 131, 187–194.

Fleming, L.E., Kirkpatrick, B., Backer, L.C., Walsh, C.J., Nierenberg, K., Clark, J., Reich, A., Hollenbeck, J., Benson, J., Cheng, Y.S., et al., 2011. Review of Florida red tide and human health effects. Harmful Algae 10, 224–233.

Hardison, D.R., Holland, W.C., Currier, R.D., Kirkpatrick, B., Stumpf, R., Fanara, T., Burris, D., Reich, A., Kirkpatrick, G.J., Litaker, R.W., 2019. HABscope: a tool for use by citizen scientists to facilitate early warning of respiratory irritation caused by toxic blooms of *Karenia brevis*. PLOS ONE 14, 1–17.

Hawkes, A.G., 1971. Spectra of some self-exciting and mutually exciting point processes. Biometrika 58, 83–90.

Kirkpatrick, B., Bean, J., Fleming, L.E., Backer, L.C., Akers, R., Wanner, A., Dalpra, D., Nierenberg, K., Reich, A., Baden, D., 2009. Aerosolized red tide toxins (brevetoxins) and asthma: a 10 day follow up after 1 h acute beach exposure. Proceedings of the 12th International Conference on Harmful Algae, pp. 297–299.

Kirkpatrick, B., Currier, R., Nierenberg, K., Reich, A., Backer, L.C., Stumpf, R., Fleming, L., Kirkpatrick, G., 2008. Florida red tide and human health: a pilot beach conditions reporting system to minimize human exposure. Sci. Total Environ. 402, 1–8.

Kirkpatrick, B., Fleming, L.E., Backer, L.C., Bean, J.A., Tamer, R., Kirkpatrick, G., Kane, T., Wanner, A., Dalpra, D., Reich, A., et al., 2006. Environmental exposures to Florida red tides: effects on emergency room respiratory diagnoses admissions. Harmful Algae 5, 526–533.

Kirkpatrick, B., Fleming, L.E., Bean, J.A., Nierenberg, K., Backer, L.C., Cheng, Y.S., Pierce, R., Reich, A., Naar, J., Wanner, A., Abraham, W., Zhou, Y., Hollenbeck, J., Baden, D., 2011. Aerosolized red tide toxins (brevetoxins) and asthma: continued health effects after 1 h beach exposure. Harmful Algae 10, 138–143.

Kirkpatrick, B., Kohler, K., Byrne, M., Fleming, L.E., Scheller, K., Reich, A., Hitchcock, G., Kirkpatrick, G., Ullmann, S., Hoagland, P., 2014. Human responses to Florida red tides: Policy awareness and adherence to local fertilizer ordinances. Sci. Total Environ. 493, 898–909.

Laub, P. J., Taimre, T., & Pollett, P. K. (2015). Hawkes processes. arXiv preprint arXiv:1507.02822.

Moeltner, K., Fanara, T., Foroutan, H., Hanlon, R., Lovko, V., Ross, S., Scgmale III, D.S., 2021. Harmful algal blooms and toxic air: the economic value of improved forecasts. Marine Resource Econ.

Mohler, G.O., Short, M.B., Brantingham, P.J., Schoenberg, F.P., Tita, G.E., 2011. Self-exciting point process modeling of crime. J. Am. Stat. Assoc. 106, 100–108.

Mote Marine Laboratory & Aquarium (2021). Beach conditions reporting system. Web site: https://www.visitbeaches.org/; last accessed Jan. 14, 2021.

National Oceanic and Atmospheric Administration (2021). Harmful algal bloom operational forecast system. Web site: https://www.tidesandcurrents.noaa.gov/hab/gomx.html/; last accessed May 19, 2021.

Nelder, J.A., Mead, R., 1965. A simplex method for function minimization. Comput. J. 7, 308–313.

Nierenberg, K., Byrne, M.M., Fleming, L.E., Stephan, W., Reich, A., Backer, L.C., Tanga, E., Dalpra, D.R., Kirkpatrick, B., 2010a. Florida red tide perception: residents versus tourists. Harmful Algae 9, 600–606.

Nierenberg, K., Hollenbeck, J., Fleming, L.E., Stephan, W., Reich, A., Backer, L.C., Currier, R., Kirkpatrick, B., 2011. Frontiers in outreach and education: the Florida red tide experience. Harmful Algae 10, 374–380.

Nierenberg, K., Kirner, K., Hoagland, P., Ullmann, S., LeBlanc, W.G., Kirkpatrick, G., Fleming, L.E., Kirkpatrick, B., 2010b. Changes in work habits of lifeguards in relation to Florida red tide. Harmful Algae 9, 419–425.

Nierenberg, K., Reich, A., Currier, R., Kirkpatrick, B., Backer, L.C., Stumpf, R., Fleming, L., Kirkpatrick, G., 2009. Beaches and HABs: successful expansion of the Florida red tide reporting system for protection of public health through community education and outreach. Florida J. Environ. Health 18–24.

Ogata, Y., 1988. Statistical models for earthquake occurrences and residual analysis for point processes. J. Am. Stat. Assoc. 83, 9–27.

Ozaki, T., 1979. Maximum likelihood estimation of Hawkes' self-exciting point processes. Ann. Inst. Stat.Math. 31, 145–155.

Park, J., Schoenberg, F.P., Bertozzi, A.L., Brantingham, P.J., 2021. Investigating clustering and violence interruption in gang-related violent crime data using spatial-temporal point processes with covariates. J. Am. Stat. Assoc. 0, 1–14.

Pietsch, R.B., Grothe, H., Hanlon, R., Powers, C.W., Jung, S., Ross, S.D., Schmale III, D.G., 2018. Wind-driven spume droplet production and the transport of *pseudomonas syringae* from aquatic environments. PeerJ 6, e5663.

Stumpf, R., Culver, M., Tester, P., Tomlinson, M., Kirkpatrick, G., Pederson, B., Truby, E., Ransibrahmanakul, V., Soracco, M., 2003. Monitoring Karenia brevis blooms in the Gulf of Mexico using satellite ocean color imagery and other data. Harmful Algae 2, 147–160.

Stumpf, R.P., Tomlinson, M.C., Calkins, J.A., Kirkpatrick, B., Fisher, K., Nierenberg, K., Currier, R., Wynne, T.T., 2009. Skill assessment for an operational algal bloom forecast system. J. Marine Syst. 76, 151–161.

System, G. o. M. C. O. O. (2021). Experimental red tide respiratory forecast. Web site: https://www.habforecast.gcoos.org/; last accessed May 19, 2021.

Türkyilmaz, K., van Lieshout, M.N.M., Stein, A., 2013. Comparing the Hawkes and trigger process models for aftershock sequences following the 2005 Kashmir earthquake. Math. Geosci. 45, 149–164.

Vargo, G.A., Heil, C.A., Fanning, K.A., Dixon, L.K., Neely, M.B., Lester, K., Ault, D., Murasko, S., Havens, J., Walsh, J., Bell, S., 2008. Nutrient availability in support of *Karenia brevis* blooms on the central West Florida shelf: what keeps Karenia blooming? Cont. Shelf Res. 28, 73–98.

Veen, A., Schoenberg, F.P., 2008. Estimation of space-time branching process models in seismology using an EM-type algorithm. J. Am. Stat. Assoc. 103, 614–624.